Wavelet and Finite Element Solutions for the Neumann Problem Using Fictitious Domains

Roland Glowinski
T. W. Pan
Raymond O. Wells, Jr.
Xiaodong Zhou

March 10, 1994

Contents

1 Introduction

The Neumann problem in two dimensions is a classical test case for any elliptic solver. In this paper we bring together several new ideas and compare them with more classical techniques. There are several fundamental ingredients coming together here:

- The boundary value problem is formulated for an open domain with a rectifiable boundary of any shape.
- The given domain is embedded in a larger and simpler domain (usually rectilinear in shape).
- The elliptic boundary-value problem in the original domain is reformulated in a weak form as an integral equation in the larger domain, and this involves introducing a regularization parameter ϵ (the so-called penalty parameter). Solutions depending on ϵ converge to solutions of the original equation as ϵ converges to zero.
- Both wavelet and finite-element Galerkin type methods are used for numerical approximations in the larger domain for fixed and small values of ϵ.
- Due to the rectilinear nature of the larger domain, fast periodic solvers can be implemented in the larger domain.

Earlier work on fictitious domains is discussed in the sections below. In Section 2 we discuss the variational formulation of the Neumann problem which will set the framework for the rest of the paper. In Section 3 we formulate the fictitious domain extension of our boundary-value problem to a larger simpler domain and prove a convergence theorem which asserts that as the penalty parameter ϵ tends to zero the regularized solution of the problem u_ϵ converges to a solution of the boundary-value problem. In Section 4, we consider the finite element approximation of the regularized Neumann problem and the error estimate of the finite element solution.

2 The Neumann Problem for Elliptic Operators: Variational Formulations

2.1 Generalities

Let ω be an open connected set (i.e., a domain) of $\mathbf{R}^d, (d \geq 1)$, and let us denote by γ the boundary $\partial\omega$ of ω. Various applications from physics, mechanics, and engineering lead one to consider the solution of the following problem:

$$-\nabla \cdot \mathbf{A}\nabla u + a_0 u = f \quad in \quad \omega, \tag{2.1}$$

$$\mathbf{A}\nabla u \cdot \mathbf{n} = g \quad on \quad \partial\omega. \tag{2.2}$$

In (2.1), (2.2) we use the standard notation

$$\nabla = \left\{ \frac{\partial}{\partial x_i} \right\}_{i=1}^{d},$$

where $x = \{x_i\}_{i=1}^d$ is the generic point in $\mathbf{R}^d$. Moreover, we set

$$\nabla \cdot \mathbf{V} = \sum_{i=1}^{d} \frac{\partial V_i}{\partial x_i}, \qquad \mathbf{a} \cdot \mathbf{b} = \sum_{i=1}^{d} a_i b_i,$$

where $\mathbf{V} = \{V_i\}_{i=1}^d$ is a vector-valued function, $\mathbf{a} = \{a_i\}_{i=1}^d, \mathbf{b} = \{b_i\}_{i=1}^d$ are vectors in $\mathbf{R}^d$ (distinguishing between vectors and points in $\mathbf{R}^d$ in this context for clarity), and where $\mathbf{n}$ is the unit vector of the outward normal to $\partial\omega$ at a generic point. In addition we assume positivity properties of the coefficients to make it an elliptic problem. Namely, we assume that

$$a_0 \in L^\infty(\omega), a_0(x) \geq 0, \text{a.e. on } \omega, a_0 \neq 0, \tag{2.3}$$

and, moreover, that, $\mathbf{A}$ is a $d \times d$ matrix whose entries a_{ij} belong to $L^\infty(\omega)$ and which satisfies the following ellipticity property

$$\mathbf{A}(x)\xi \cdot \xi \geq \alpha|\xi|^2, \quad \text{a.e. on } \omega, \quad \forall \xi \in \mathbf{R}^d, \tag{2.4}$$

where, in (2.4), α is a *positive* constant and $|\xi|^2 = \xi \cdot \xi$. Finally we assume that the input data f and g satisfy regularity conditions of the form:

$$f \in L^2(\omega), g \in H^{-\frac{1}{2}}(\partial\omega). \tag{2.5}$$

Remark: We can take for f mathematical objects which are much less regular than a $L^2(\omega)$-function. For example, f can be a measure supported by a $(d-1)$-manifold contained into ω. In fact, the various methods to be described in the following parts of this article will apply to these situations.

The main goal of this article is to discuss a solution methodology for problem (2.1), (2.2) based on the so-called fictitious (or imbedding) domain concept; fictitious domain formulations (to be described in Section 3) heavily rely on the variational formulations for the Neumann problem (2.1), (2.2) to be discussed in the next section.

2.2 Variational Formulation of the Neumann Problem

Following, e.g., [7], we derive a *variational formulation* of problem (2.1) by multiplying both sides of equation (2.1) by $v \in H^1(\omega)$, and then applying the *divergence theorem.* We obtain then (with $dx = dx_1 \ldots dx_d$)

$$\begin{aligned} & \int_\omega (-\nabla \cdot \mathbf{A}\nabla uv + a_0 uv)dx \\ = & \int_\omega (\mathbf{A}\nabla u \cdot \nabla v + a_0 uv)dx - \int_{\partial\omega} \mathbf{A}\nabla u \cdot \mathbf{n} v d\gamma \\ = & \int_\omega fvdx, \end{aligned}$$

where $d\gamma$ is the induced Lebesgue measure on $\partial\omega$. Combining this with (2.2) implies that u satisfies (at least formally)

$$\int_\omega (\mathbf{A}\nabla u \cdot \nabla v + a_0 uv)dx = \int_\omega fvdx + \langle g, v\rangle, \quad \forall v \in H^1(\omega), \tag{2.6}$$

where $\langle \cdot, \cdot \rangle$ denotes the duality pairing between $H^{-\frac{1}{2}}(\partial\omega)$ and $H^{\frac{1}{2}}(\partial\omega)$. Relation (2.6) is at the basis of a classical *variational formulation* of the Neumann problem, since it can be shown that if a function $u \in H^1(\omega)$ satisfies (2.6) then it is also a solution of problem (2.1), (2.2), the derivatives in (2.1) being taken in the distribution sense. The variational formulation of (2.1), (2.2) derived from (2.6) becomes

$$\begin{cases} \text{Find } u \in H^1(\omega) \textit{ such that } \forall v \in H^1(\omega) \textit{ we have} \\ \int_\omega (\mathbf{A}\nabla u \cdot \nabla v + a_0 uv)dx = \int_\omega fv dx + \langle g, v \rangle. \end{cases} \tag{2.7}$$

It is shown in, e.g., [7] that problem (2.7) has (as a consequence of the *Lax-Milgram lemma*) a *unique* solution if (2.3)-(2.5) hold.

Formulation (2.7) is at the basis of powerful *Galerkin-type* solution methods such as *finite elements* (see, e.g., [12,7,2,1]). In this article, we shall combine it with fictitious domain techniques in order to derive solution methods well suited to wavelet and finite element approximations taking advantage of Cartesian meshes.

3 Fictitious Domain Formulations of the Neumann Problem

3.1 A Basic Fictitious Domain Formulation

In order to solve the Neumann problem (2.1), (2.2) we imbed ω in a larger domain Ω (see Figure 3.1 for an illustration of such a situation).

In the following parts of this article, we shall assume that Ω is a d-dimensional "box", that is, Ω is a product of intervals (as illustrated in Figure 3.1 for $d = 2$). We consider then a closed subspace V of $H^1(\Omega)$ such that

$$\{v : v = \tilde{v}|_\omega, \tilde{v} \in V\} = H^1(\omega). \tag{3.8}$$

Typical choices for V are $H^1(\Omega)$, $H_0^1(\Omega)$ and the space $V_P(\Omega)$ defined by

$$V_P(\Omega) = \{v \in H^1(\Omega) : v \text{ is periodic on } \partial\Omega\}. \tag{3.9}$$

Suppose that $\Omega = (0, L)^d$ for some $L > 0$. Then the periodicity property in (3.9) means that $v(0, x_2, \ldots, x_d) = v(L, x_2, \ldots, x_d)$ for almost every

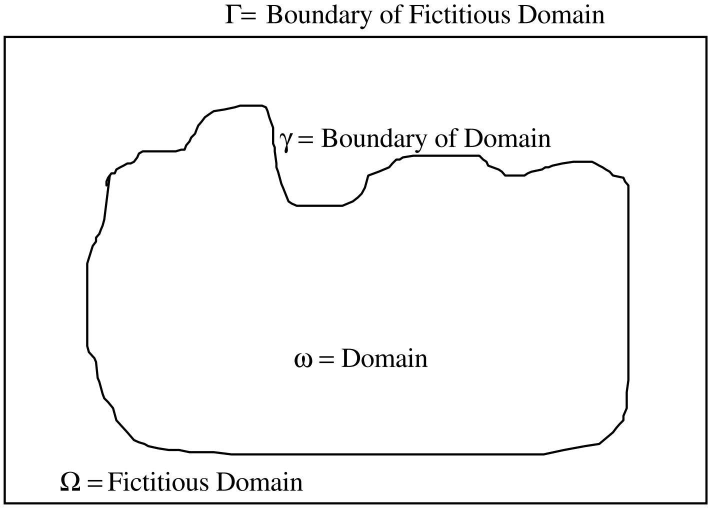

Figure 3.1: Imbedding of ω in Ω

$\{x_2, \ldots, x_d\} \in (0, L)^{d-1}$ with similar relations for the other $d-1$ axis of co-ordinates directions. Next, we introduce a bilinear form $b : V \times V \to \mathbf{R}$ and a linear functional $L : V \to \mathbf{R}$, such that $b(\cdot, \cdot)$ is continuous and V-elliptic over $V \times V$, and L is continuous over V.

We can, for example, define b by

$$b(v, w) = \int_\Omega (b_0 v w + \mathbf{B} \nabla v \cdot \nabla w) dx, \quad \forall v, w \in V, \tag{3.10}$$

where $b_0 \in L^\infty(\Omega), b_0 \geq 0, b \neq 0$, and where

$$\mathbf{B} \in L^\infty(\mathbf{R}^{d^2}), \qquad \mathbf{B}(x)\xi \cdot \xi \geq \beta |\xi|^2, \quad \text{a.e. on } \Omega \quad \forall \xi \in \mathbf{R}^d,$$

with β a positive constant. Actually, if $V = H_0^1(\Omega)$, we can take $b_0 = 0$; the properties of $\mathbf{B}$ imply that $b(\cdot, \cdot)$ is still strongly elliptic over $H_0^1(\Omega) \times H_0^1(\Omega)$.

Remark: The functions b_0 and $\mathbf{B}$ restricted to ω may coincide with a_0 and $\mathbf{A}$ but this is not a necessity; similarly, it is not necessary to have L related to f and g. Therefore $L = 0$ is a possible choice.

Next, we introduce the following subspaces of V:

$$\begin{aligned} H &= \{v \in V : \int_\omega (a_0 v\mu + \mathbf{A}\nabla v \cdot \nabla \mu)dx = \\ &\qquad \int_\omega f\mu dx + \langle g, \mu\rangle, \forall \mu \in V\} \qquad (3.11) \\ H_0 &= \{v \in V : \int_\omega (a_0 v\mu + \mathbf{A}\nabla v \cdot \nabla \mu)dx = 0, \quad \forall \mu \in V\} \qquad (3.12) \end{aligned}$$

Assuming that the hypothesis on $a_0, \mathbf{A}, f, g$ made in Section 2.2 hold, the Neumann problem (2.1), (2.2), or its variational formulation (2.7), has a unique solution; this fact combined with the inclusion hypothesis (3.8) implies that H is *nonempty*; in addition we clearly have that H is a *closed convex* subset of V. Similar properties hold for H_0 which is therefore a nonempty closed subspace of V. We consider next the following problem

$$\begin{cases} \tilde{u} \in H, \\ b(\tilde{u}, v - \tilde{u}) \geq L(v - \tilde{u}), \quad \forall v \in H. \end{cases} \qquad (3.13)$$

Problem (3.13) is a classical variational inequality like those discussed in, e.g., [10,7,8]. It follows from the above references that the properties of $b(\cdot,\cdot), L(\cdot)$ and H imply that problem (3.13) has a unique solution. Also, since $\tilde{u} + w \in H, \quad \forall w \in H_0$, we obtain from (3.13) (taking $v = \tilde{u} + w$) that

$$b(\tilde{u}, w) \geq L(w), \quad \forall w \in H_0,$$

which implies in turn (since $-w$ also belongs to H_0) that

$$b(\tilde{u}, w) = L(w), \quad \forall w \in H_0.$$

We have thus shown that the solution of (3.13) is necessarily the solution of

$$\begin{cases} \tilde{u} \in H, \\ b(\tilde{u}, v) = L(v), \quad \forall v \in H_0. \end{cases} \qquad (3.14)$$

The reciprocal property is obviously true since

$$b(\tilde{u}, v) = L(v); \quad \forall v \in H_0 \quad \text{implies} \quad b(\tilde{u}, v - \tilde{u}) = L(v - \tilde{u}), \quad \forall v \in H,$$

which implies in turn

$$b(\tilde{u}, v - \tilde{u}) \geq L(v - \tilde{u}), \quad \forall v \in H.$$

It is also obvious that

$$\tilde{u} \mid_\omega = u \qquad (3.15)$$

where, in (3.15), u is the solution of problem (2.1), (2.2), (2.7).

3.2 A Regularization and Fictitious Domain Method

In this paragraph, we shall use the following notation:

$$a(v,w) = \int_\omega (A\nabla v \cdot \nabla w + a_0 vw)dx, \quad \forall v,w \in V, \tag{3.16}$$

$$l(v) = \int_\omega fvdx + \langle g, v\rangle, \quad \forall v \in V. \tag{3.17}$$

We consider then the following linear variational problem:

$$\begin{cases} u_\epsilon \in V, \\ \epsilon b(u_\epsilon, v) + a(u_\epsilon, v) = \epsilon L(v) + l(v), \quad \forall v \in V, \end{cases} \tag{3.18}$$

where, in (3.18), ϵ is a *positive* parameter. Then we have the following convergence theorem.

Theorem 3.1 *Suppose that ω is a $C^{0,1}$ domain; suppose also that the above hypotheses on a, b, l, L hold. We have then*

$$\lim_{\epsilon\to 0}\|u_\epsilon - \tilde{u}\|_{H^1(\Omega)} = 0, \tag{3.19}$$

$$\lim_{\epsilon\to 0}\epsilon^{-\frac{1}{2}}\|u_\epsilon - u\|_{H^1(\omega)} = 0, \tag{3.20}$$

where u, $\tilde{u}$, and u_ϵ are the solutions of problems (2.1), (2.2), (3.13), and (3.18), respectively.

Proof: In the following C will denote various constants.

(1) *Boundedness of $\{u_\epsilon\}_{\epsilon>o}$*: Let $\tilde{u}$ be the solution of problem (3.13); taking $v = u_\epsilon - \tilde{u}$ in (3.18) we obtain

$$\epsilon b(u_\epsilon - \tilde{u}, u_\epsilon - \tilde{u}) + a(u_\epsilon - \tilde{u}, u_\epsilon - \tilde{u}) = \epsilon[L(u_\epsilon - \tilde{u}) - b(\tilde{u}, u_\epsilon - \tilde{u})] + l(u_\epsilon - \tilde{u}) - a(\tilde{u}, u_\epsilon - \tilde{u}). \tag{3.21}$$

Since $\tilde{u}\mid_\omega = u$ it follows from (2.7), (3.11), (3.13), (3.16), and (3.17) that

$$a(\tilde{u}, v) = l(v), \quad \forall v \in V. \tag{3.22}$$

Taking $v = u_\epsilon - \tilde{u}$ in (3.22) and combining with (3.21) we obtain

$$b(u_\epsilon - \tilde{u}, u_\epsilon - \tilde{u}) + \frac{1}{\epsilon}a(u_\epsilon - \tilde{u}, u_\epsilon - \tilde{u}) = L(u_\epsilon - \tilde{u}) - b(\tilde{u}, u_\epsilon - \tilde{u}). \tag{3.23}$$

It follows from (3.23), from $\epsilon > 0$ and from the ellipticity and continuity properties of a, b, L that

$$\beta' \|u_\epsilon - \tilde{u}\|_V^2 \leq (\|L\| + \|b\| \|\tilde{u}\|_V) \|u_\epsilon - \tilde{u}\|_V, \quad \forall \epsilon > 0, \tag{3.24}$$

where, in (3.24), $\beta' > 0$ and where $\|L\|$ and $\|b\|$ are defined by

$$\|L\| = \sup_v \frac{| L(v) |}{\|v\|_V}, \quad v \in V \backslash \{0\},$$

and

$$\|b\| = \sup_{v,w} \frac{| b(v,w) |}{\|v\|_V \|w\|_V}, \quad v \in V \backslash \{0\}, \quad w \in V \backslash \{0\}.$$

Relation (3.24) implies

$$\|u_\epsilon - \tilde{u}\|_V \leq C, \quad \forall \epsilon > 0,$$

which implies in turn

$$\|u_\epsilon\|_{H^1(\Omega)} \leq C, \quad \forall \epsilon > 0 \tag{3.25}$$

□

(2) *Weak convergence of* $\{u_\epsilon\}_{\epsilon > 0}$: It follows from (3.25), and from the closedness of V in $H^1(\Omega)$ (which implies the weak closedness) that there exist $u^\star \in V$ and a subsequence - still denoted by $\{u_\epsilon\}_{\epsilon > 0}$ - such that

$$\lim_{\epsilon \to 0} u_\epsilon = u^* \quad \text{weakly in} \quad H^1(\Omega). \tag{3.26}$$

Combining (3.26) to (3.18) we obtain at the limit in (3.18) that

$$a(u^*, v) = l(v), \quad \forall v \in V,$$

i.e.,

$$u^* \in H \tag{3.27}$$

Replacing v by $v - u_\epsilon$ in (3.18) we obtain (taking into account the ellipticity of $a(\cdot, \cdot)$)

$$\begin{aligned} b(u_\epsilon, v) \quad = \quad & L(v - u_\epsilon) + b(u_\epsilon, u_\epsilon) \\ & + \frac{1}{\epsilon} a(u_\epsilon, u_\epsilon) + \frac{1}{\epsilon} \left[l(v - u_\epsilon) - a(v, v - u_\epsilon) \right] \\ & \geq L(v - u_\epsilon) + b(u_\epsilon, u_\epsilon) \\ & + \frac{1}{\epsilon} \left[l(v - u_\epsilon) - a(v, v - u_\epsilon) \right], \quad \forall v \in V. \end{aligned} \tag{3.28}$$

Suppose now that $v \in H$; we have then $v \mid_{\omega} = u$ which implies that

$$a(v, v - u_\epsilon) = l(v - u_\epsilon), \quad \forall v \in H,$$

which combined to (3.28) implies in turn that

$$b(u_\epsilon, v) \geq L(v - u_\epsilon) + b(u_\epsilon, u_\epsilon), \quad \forall v \in H. \tag{3.29}$$

Since $b(\cdot, \cdot)$ is positive definite over $V \times V$ we have, from (3.26),

$$\liminf_{\epsilon \to 0} b(u_\epsilon, u_\epsilon) \geq b(u^*, u^*),$$

which combined to (3.29) implies

$$b(u^*, v) \geq L(v - u^*) + b(u^*, u^*), \quad \forall v \in H.$$

We have thus proved (taking (3.27) into account) that u^* is a solution of (3.13); since (3.13) has a unique solution we have $u^* = \tilde{u}$, which implies that the whole family $\{u_\epsilon\}_{\epsilon > 0}$ converges to $\tilde{u}$. □

(3) *Strong convergence of* $\{u_\epsilon\}_{\epsilon>0}$: Consider relation (3.23); we have just shown that u_ϵ converges weakly to $\tilde{u}$. Combining this result with (3.23), and taking into account the ellipticity properties of $a(\cdot, \cdot)$ and $b(\cdot, \cdot)$, we finally obtain the convergence properties (3.19), (3.20). □

4 Wavelet and Finite Element-Galerkin Solution of the Neumann Problem

4.1 Numerical Approximations

In this section we want to formulate a Galerkin solution of the regularized Neumann problem as posed in (2.7), Section 3, where A and B are identity matrices and $a_0 = b_0 = \alpha > 0$.

Let V_h be a finite dimensional subspace of V. We have

$$\begin{cases} \text{Find } u_h^\epsilon \text{ in } V_h \text{ such that} \\ a(u_h^\epsilon, v_h) + \epsilon b(u_h^\epsilon, v_h) = \epsilon L(v_h) + l(v_h), \quad \forall v_h \in V_h. \end{cases} \tag{4.30}$$

Problem (4.30) has a unique solution in V_h.

4.2 Error Estimates

In this section, we assume that ω is $C^{1,1}$ domain and $f \in L^2(\omega), g \in H^{\frac{1}{2}}(\partial\omega)$. Then the solution u of problem (2.7) is in $H^2(\omega)$. In order to get error estimates for $\|u - u_h^\epsilon\|_{H^1(\omega)}$ and $\|u - u_h^\epsilon\|_{L^2(\omega)}$, we need to extend the solution u of problem (2.7) from $H^2(\omega)$ into V. In [4], there is a basic extension result. We state it in the following

Theorem 4.1 *Let ω be a bounded domain in $\mathbf{R}^d$ with a $C^{k,1}$ boundary for some integer $k \geq 0$ and $\omega \subset\subset \Omega$ where Ω is an open set. Then there is a bounded linear extension operator E from $H^{k+1}(\omega)$ into $H_0^{k+1}(\Omega)$ such that $Ev|_\omega = v$ and*

$$\|Ev\|_{H^{k+1}(\Omega)} \leq C(k, \omega, \Omega)\|u\|_{H^{k+1}(\omega)} \tag{4.31}$$

for all $v \in H^{k+1}(\omega)$.

Thus for the polygonal fictitious domain Ω, $\omega \subset\subset \Omega$, we can extend the solution u of the problem (2.7) from $H^2(\omega)$ to $H_0^2(\Omega)$, and especially for square domain Ω, we can extend u from $H^2(\omega)$ to $H_p^2(\omega)$, the space of periodic functions in $H^2(\Omega)$. Let the extension u be denoted by Eu. We have the following result [5]

Lemma 4.2 *Assume that ω is a bounded domain in $\mathbf{R}^d$ with a $C^{1,1}$ boundary and $\omega \subset\subset \Omega$ where Ω is a polygonal domain. Then there exists a constant C_1 such that*

$$\|u_h^\epsilon - u\|_{H^1(\omega)} \leq C_1 \inf_{v_h \in V_h}\{\|Eu - v_h\|^2_{H^1(\Omega)} + \epsilon\|\tilde{f}\|^2_{L^2(\Omega)} + \epsilon\|Eu\|^2_{H^1(\Omega)}\}^{\frac{1}{2}}, \tag{4.32}$$

where u is the solution of problem (2.7) and u_h^ϵ is the solution of problem (4.30).

4.3 Finite Element Discretization

Let us give a brief description of the finite element spaces used to obtain the error estimates in the following. Let $\mathcal{T}_h$ be a regular triangulation of the polygonal domain Ω. We would like to use finite elements, d–simplices of type (k), for integer $k > 0$ (other finite elements can be used). The finite element spaces V_h associated with the finite elements d–simplices of type (k) are given by

$$V_h := \{v_h : v_h \in H_0^1(\Omega) \cap \mathbf{C}^0(\bar{\Omega}), v_h|_T \in P_k, \forall T \in \mathcal{T}_h\}$$

where P_k is the space of the polynomials in n variables of degree $\leq k$.

Let $\{\psi_i\}_{i=1}^N$ be the basis of the finite element space V_h where N is the dimension of V_h and $\{d_i\}_{i=1}^N$ is the set of the mesh nodes; it satisfies the following relation

$$\psi_i(d_j) = \delta_{ij} = \begin{cases} 1, & i = j, \\ 0, & i \neq j, \end{cases}$$

for $1 \leq i, j \leq N$. Also for any v_h in V_h, we have

$$v_h = \sum_{i=1}^N v_h(d_i)\psi_i.$$

The V_h–interpolant is defined by

$$\Pi_h v = \sum_{i=1}^N v(d_i)\psi_i,$$

for any $v \in C^0(\bar{\Omega})$. There are estimates of the interpolation error in [2]. We will use the following

Theorem 4.3 *If $k > \dfrac{d}{2} - 1$, then there exists a constant C_2 independent of h such that, for any function $v \in H^{k+1}(\Omega) \cap H_0^1(\Omega)$,*

$$\|v - \Pi_h v\|_{H^1(\Omega)} \leq C_2 h^k \|v\|_{H^{k+1}(\Omega)}. \tag{4.33}$$

Let us assume that the solution u of problem (2.7) verifies $u \in H^{k+1}(\omega)$ for an integer $k > \max\{0, \dfrac{d}{2} - 1\}$. Suppose also that ω is a bounded domain with a $C^{k,1}$ boundary, strictly contained in the polygonal open set Ω. We obtain the following H^1 error estimate ([5]).

Theorem 4.4 *Let ω be a bounded domain in $\mathcal{R}^d$ with a $C^{k,1}$ boundary for integer $k > \max\{0, \frac{d}{2} - 1\}$, strictly contained in the polygonal open set Ω.*

If the solution u of problem (2.7) verifies $u \in H^{k+1}(\omega)$, then there exists a constant C_3 independent of h such that

$$\|u_h^\epsilon - u\|_{H^1(\omega)} \leq C_3\{h^k\|u\|_{H^{k+1}(\omega)} + \sqrt{\epsilon}\|\tilde{f}\|_{L^2(\Omega)} + \sqrt{\epsilon}\|u\|_{H^{k+1}(\omega)}\}, \quad (4.34)$$

where u_h^ϵ is the solution of problem (4.30) and $\epsilon > 0$.

Therefore the optimal choice of ϵ is $\epsilon = Mh^{2s}$ where M is constant and $s \geq k$ so that $\|u - u_h^\epsilon\|_{H^1(\omega)}$ is of order h^k.

For the L^2 error estimate, we consider the following auxiliary problem:

$$\left\{ \begin{array}{l} \text{Find } \phi \text{ in } H^1(\omega) \text{ such that} \\ \displaystyle\int_\omega (\alpha\phi v + \nabla\phi \cdot \nabla v)\, dx = \int_\omega (u - u_h^\epsilon) v\, dx, \quad \forall v \in H^1(\omega), \end{array} \right. \quad (4.35)$$

Since $u - u_h^\epsilon \in H^1(\omega)$, we have

$$\|\phi\|_{H^2(\omega)} \leq C_5 \|u - u_h^\epsilon\|_{L^2(\omega)}. \quad (4.36)$$

Also we consider the auxiliary problem with fictitious domain penalty approach:

$$\left\{ \begin{array}{l} \text{Find } \phi^\rho \text{ in } H_0^1(\Omega) \text{ such that} \\ a(\phi^\rho, v) + \rho b(\phi^\rho, v) = \displaystyle\int_\omega (u - u_h^\epsilon) v\, dx, \quad \forall v \in H_0^1(\Omega). \end{array} \right. \quad (4.37)$$

and the finite element approximation of problem (4.37)

$$\left\{ \begin{array}{l} Find\ \psi_h^\rho\ in\ V_h\ such\ that \\ a(\psi_h^\rho, v_h) + \rho b(\psi_h^\rho, v_h) = \displaystyle\int_\omega (u - u_h^\epsilon) v_h\, dx, \forall v_h \in V_h. \end{array} \right. \quad (4.38)$$

Problems (4.37) and (4.38) have a unique solution in $H_0^1(\Omega)$ and V_h respectively.

The L^2 error estimate is obtained from the following result ([5]).

Theorem 4.5 *Assume that the conditions in Theorem 4.4 hold and $d \leq 3$. Then there exists a constant C_4 independent of h such that*

$$\|u - u_h^\epsilon\|_{L^2(\omega)} \leq C_4 \Big\{ \left(h + \sqrt{\rho}\right) \left((h^k + \sqrt{\epsilon})\|u\|_{H^{k+1}(\omega)} + \sqrt{\epsilon}\|\tilde{f}\|_{L^2(\Omega)}\right)$$
$$+\epsilon \left(\frac{h}{\sqrt{\rho}} + 1\right) \left\{ \left(\frac{h^k}{\sqrt{\epsilon}} + 1\right) \|u\|_{H^{k+1}(\omega)} + 2\|\tilde{f}\|_{L^2(\Omega)} \right\} \Big\} \quad (4.39)$$

where u is the solution of problem (2.7), u_h^ϵ *is the solution of problem* (4.30) *and* $\epsilon, \rho > 0$.

Let $\epsilon = M_1 h^{2s}$ and $\rho = M_2 h^{2l}$ where M_1, M_2 are constants and s, l are integers. Then the optimal choices of ϵ and ρ are $s \geq k$ and $s \geq l > 0$ so that $\|u - u_h^\epsilon\|_{L^2(\omega)}$ is of order h^{k+1}.

4.4 Wavelet Discretization

Let ϕ be the Daubechies scaling function of $N (N \geq 3)$, [3]. Define $\phi_{j,k} := 2^{j/2}\phi(2^j x - k)$ for $k, j \in \mathbf{Z}$. We assume $\Omega = (-s, s) \times (-s, s)$, where s is a positive integer. Set

$$V_j := \left\{ v \in L^2(\Omega) : v(x,y) = \sum_{k,l \in \mathbf{Z}} c_{k,l}\phi_{j,k}(x)\phi_{j,l}(y), \quad x \in \Omega, \quad c_{k,l} = c_{k+2^j 2s, l+2^j 2s} \right\}.$$

V_j(resp. u_j) corresponds to V_h(resp. u_h) described in Section 4.1 with $h = \frac{1}{2^j}$. Under the assumptions of Theorems 4.4 and 4.5, the analysis of [14] gives

$$\|u - u_j^\epsilon\|_{H^1(\omega)} = O\left(2^{-j} + \sqrt{\epsilon}\right)$$

and

$$\|u - u_j^\epsilon\|_{L^2(\omega)} = O\left(2^{-2j} + \sqrt{\epsilon}\right).$$

5 Numerical Experiments

5.1 Finite Element Method

We consider the following test problems. Let $\omega = \{(x,y) | x^2 + y^2 < \dfrac{1}{16}\}$ and $\Omega = (-1,1) \times (-1,1)$, and let $u(x,y) = x^2 + y^2$ (resp. $u(x,y) = x^3 - y^3$) be the solution of the following Neumann problem

$$\begin{aligned} u - \triangle u &= f \text{ in } \omega, \\ \frac{\partial u}{\partial n} &= g \text{ on } \gamma; \end{aligned}$$

we then have $f(x,y) = x^2 + y^2 - 4$ and $g(x,y) = 1/2$ (resp. $f(x,y) = x^3 - y^3 - 6(x-y)$ and $g(x,y) = 12(x^3 - y^3)$).

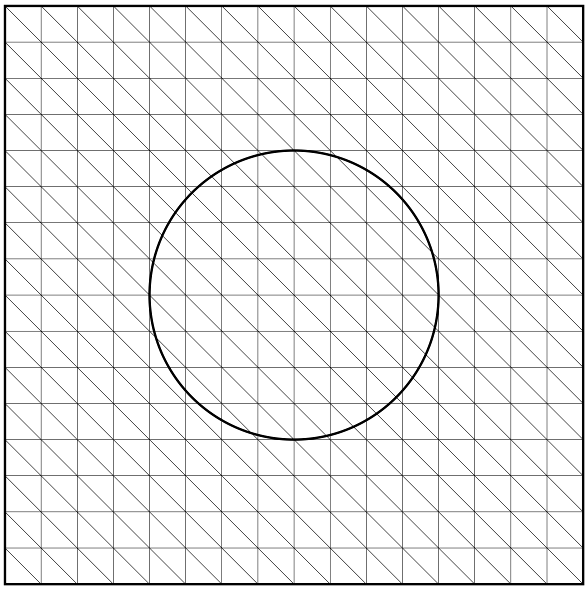

Figure 5.2: Finite element grid with mesh size $h = 1/8$

In numerical experiments, we use 2–simplices of type (1) finite elements, so

$$V_h = \{v_h : v_h \in H_0^1(\Omega) \cap \mathbf{C}^0(\bar{\Omega}), v_h|_T \in P_1, \forall T \in \mathcal{T}_h\}$$

where $\mathcal{T}_h$ is the regular uniform triangulations of Ω (e.g., see Figure 5.2) and P_1 is the space of the polynomials in 2 variables of degree 1.

The $\tilde{f}$ in (4.30) is given by $\tilde{f} = f$ in Ω. The line integral along $\partial\omega$ in (4.30) is evaluated by Simpson's composite rule. The mesh sizes are 1/8, 1/16 and 1/32. For the finite element $T \in \mathcal{T}_h$ with area$(T \cap \omega) \neq 0$ and area$(T \cap \omega) \neq$ area (T), the area $(T \cap \omega)$ has to be computed accurately enough to obtain good results. The linear systems obtained from problem (4.30) have been solved via a *Cholesky factorization*. The CPU times for solving problem (4.30) with a given ϵ on a Sparcstation 2 are 1.8 seconds, 7.6 seconds and 193.4 seconds for mesh size 1/8, 1/16 and 1/32 respectively.

For the test problem with $u(x, y) = x^3 - y^3$, we list the relative H^1 and L^2 errors with ϵ going from 10^{-1} to 10^{-10} in Tables 5.1 and 5.2. The H^1 errors are of order h, the L^2 errors being of order h^2 if ϵ is small enough. These are what we expect from Theorems 4.4 and 4.5. For the other test problem with $u(x, y) = x^2 + y^2$, errors are too good to obtain the orders of errors similar

ϵ	$h = 1/8$	$h = 1/16$	$h = 1/32$
10^{-1}	1.27759362699	1.62154953409	2.16374221811
10^{-2}	0.32358749061	0.26197911257	0.29164753716
10^{-3}	0.19417803703	$8.3662335694 \times 10^{-2}$	$5.0478305305 \times 10^{-2}$
10^{-4}	0.18043329784	$6.5094253508 \times 10^{-2}$	$2.5674105973 \times 10^{-2}$
10^{-5}	0.17899468270	$6.3208218876 \times 10^{-2}$	$2.3200437070 \times 10^{-2}$
10^{-6}	0.17884885920	$6.3018799334 \times 10^{-2}$	$2.2953287236 \times 10^{-2}$
10^{-7}	0.17883425279	$6.2999847513 \times 10^{-2}$	$2.2928574657 \times 10^{-2}$
10^{-8}	0.17883279190	$6.2997952230 \times 10^{-2}$	$2.2926103423 \times 10^{-2}$
10^{-9}	0.17883264581	$6.2997762701 \times 10^{-2}$	$2.2925856300 \times 10^{-2}$
10^{-10}	0.17883263120	$6.2997743748 \times 10^{-2}$	$2.2925831587 \times 10^{-2}$

Table 5.1: $\|u - u_h^\epsilon\|_{H^1(\omega)}/\|u\|_{H^1(\omega)}$ for $u(x, y) = x^3 - y^3$ for the finite element method

to those of $u(x, y) = x^3 - y^3$.

For the test problem with $u(x, y) = x^2 + y^2$, the surfaces graphs of the approximate solutions with $h = 1/16$ are shown in Figure 5.1 for $\epsilon = 10^{-6}$. In Figure 5.1, the left figure is the graph of u_h^ϵ and the right one is the graph of $u_h^\epsilon X_\omega$ where X_ω is the characteristic function of ω. Also in Figures 5.4, 5.5, and 5.6 the variations of $x \to u_h^\epsilon(x, 0)$ (in solid line) and $x \to u(x, 0)$ (in dotted line) are shown for $\epsilon = 1$, 10^{-3} and 10^{-6}. If $\epsilon = 1.0$, it is not surprising that the approximate solution is really far away from the exact solution in ω. As ϵ becomes smaller, the approximate solution is quite accurate on ω. Even near the boundary $\partial\omega$, the approximate solution is quite accurate.

5.2 Wavelet-Galerkin Method

Let us approximate u^ϵ by $u_L^\epsilon \in V_L, j \in \mathbf{Z}^+$, as in Section 4.4. Also we sample the characteristic function χ_ω, the functions f and extended g in V_l (l and L can be distinct). Then, by precomputing the connection coefficients

$$\Gamma_{m,n} := \int \phi_(x)\phi_m'(x)\phi_n'(x)dx,$$

ϵ	$h = 1/8$	$h = 1/16$	$h = 1/32$
10^{-1}	1.48056340340	1.32677581622	1.23291488149
10^{-2}	0.37017875130	0.21327731659	0.16603820621
10^{-3}	0.21946578156	$6.6884846802 \times 10^{-2}$	$2.8487414845 \times 10^{-2}$
10^{-4}	0.20345479970	$5.1556945153 \times 10^{-2}$	$1.4246838113 \times 10^{-2}$
10^{-5}	0.20178058788	$4.9997028789 \times 10^{-2}$	$1.2813815642 \times 10^{-2}$
10^{-6}	0.20161092886	$4.9840331005 \times 10^{-2}$	$1.2670335191 \times 10^{-2}$
10^{-7}	0.20159393549	$4.9824652763 \times 10^{-2}$	$1.2655985068 \times 10^{-2}$
10^{-8}	0.20159223587	$4.9823084852 \times 10^{-2}$	$1.2654550035 \times 10^{-2}$
10^{-9}	0.20159206590	$4.9822928061 \times 10^{-2}$	$1.2654406531 \times 10^{-2}$
10^{-10}	0.20159204898	$4.9822912381 \times 10^{-2}$	$1.2654392181 \times 10^{-2}$

Table 5.2: $\|u - u_h^\epsilon\|_{L^2(\omega)}/\|u\|_{L^2(\omega)}$ for $u(x,y) = x^3 - y^3$ for the finite-element method

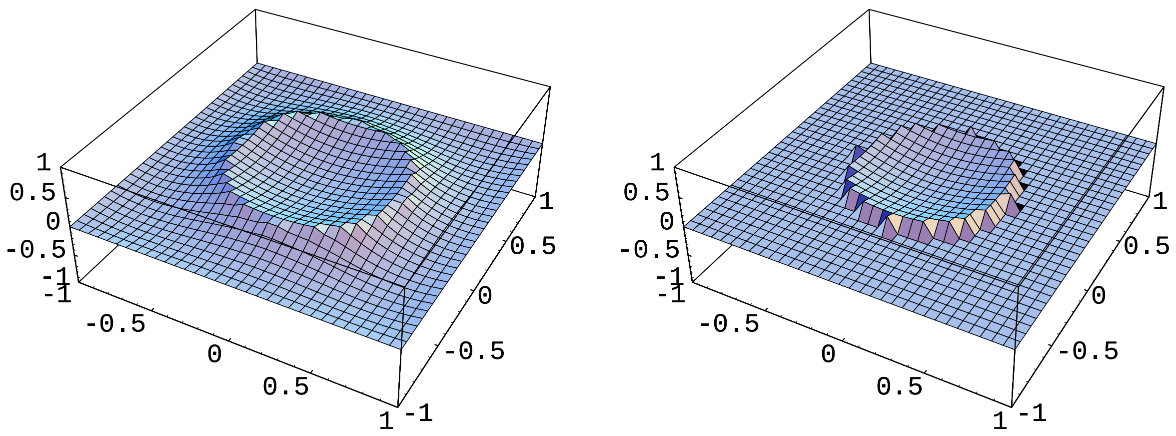

Figure 5.3: The left figure is the graph of u_h^ϵ and the right is the graph of $u_h^\epsilon X_\omega$ where X_ω is the characteristic function of ω for $\epsilon = 10^{-6}$.

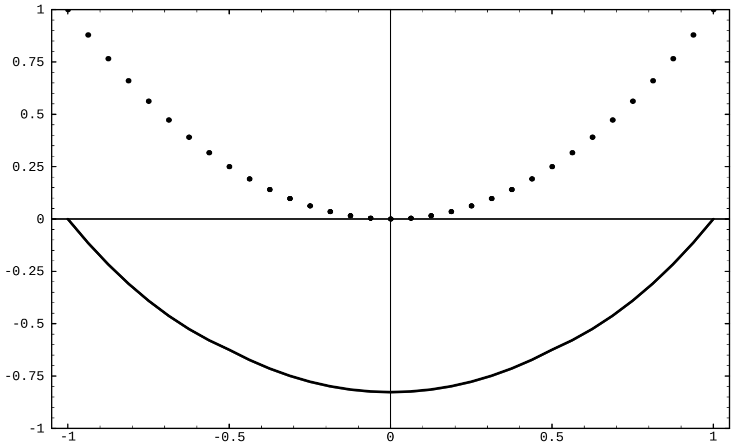

Figure 5.4: The variations of $x \to u_h^\epsilon(x,0)$ (in solid line) and $x \to u(x,0)$ (in dotted line) where $u(x,y) = x^2 + y^2$ for $\epsilon = 1.0$.

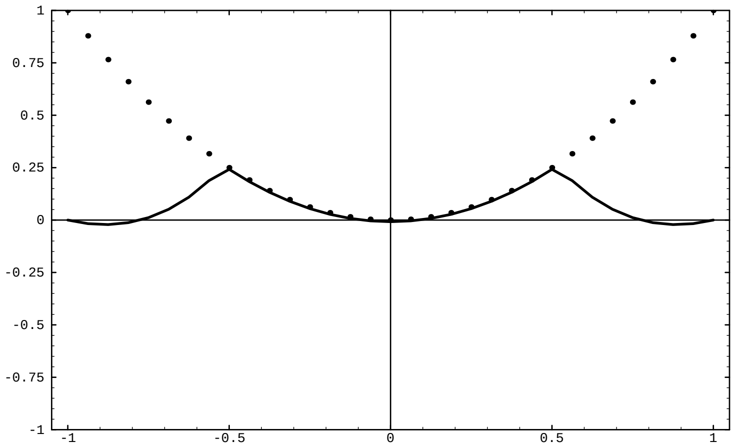

Figure 5.5: The variations of $x \to u_h^\epsilon(x,0)$ (in solid line) and $x \to u(x,0)$ (in dotted line) where $u(x,y) = x^2 + y^2$ for $\epsilon = 10^{-3}$.

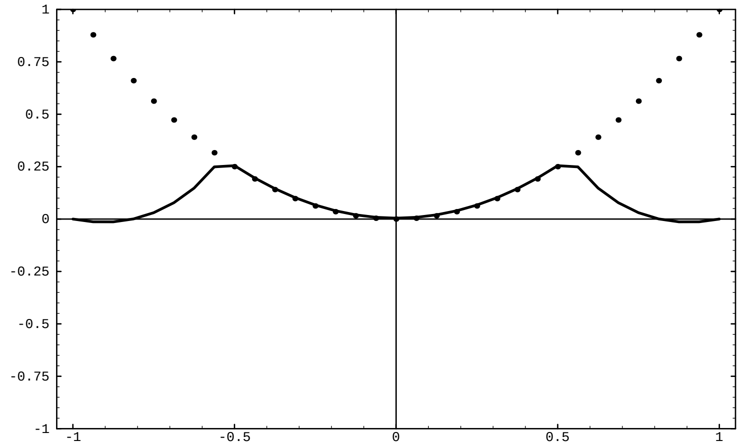

Figure 5.6: The variations of $x \to u_h^\epsilon(x,0)$ (in solid line) and $x \to u(x,0)$ (in dotted line) where $u(x,y) = x^2 + y^2$ for $\epsilon = 10^{-6}$.

one can derive the desired linear system for the unknowns.

Remark:

(1) It is convenient to choose the expansion spaces for u_L^ϵ and χ_ω to be the same to calculate

$$\int_\omega (\nabla u \nabla v + uv) dx.$$

(2) To calculate the boundary integral on the right hand side, we use the uniform geometric measure approach introduced in [13] to avoid numerical integration, since the latter required the knowledge of the parametrization of $\partial\omega$. Briefly speaking, one can write

$$\int_{\partial\omega} g ds = \int_{\mathbf{R}^2} g d\mu$$

where μ is a Radon measure supported on $\partial\omega$. In fact,

$$\mu = \nabla \chi_\omega \cdot \frac{\nabla F}{|\nabla F|} \tag{5.40}$$

if $\partial\omega$ is given by $\partial\omega = \{(x,y) : F(x,y) = 0\}$ for some Lipschitz function F. Therefore, if we sample g, χ_ω, F in V_l as $g_l, \chi_{\omega,l}, F_l$, and approximate μ by μ_l,

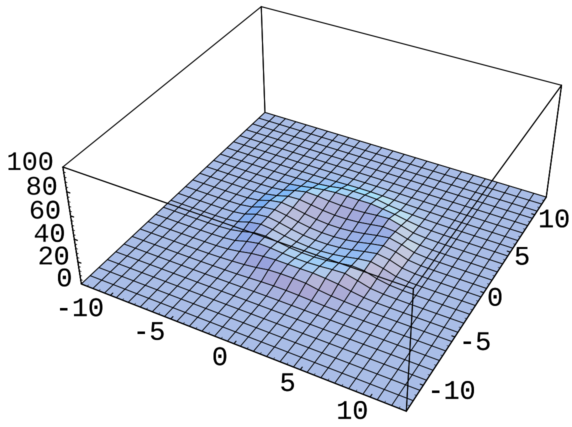

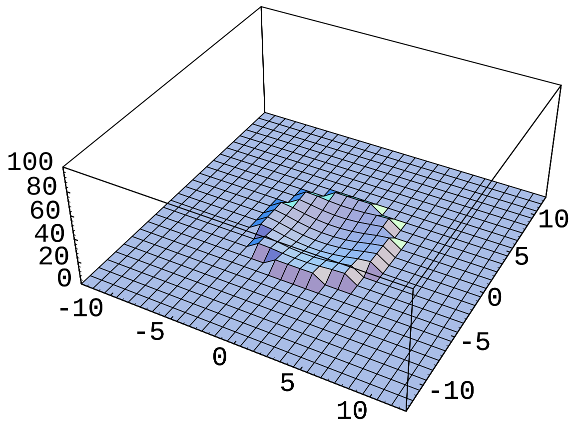

Figure 5.7: The wavelet Galerkin solution for $\epsilon = 1$.

which is calculated accordingly by the formula (5.40), one can show

$$\int_{\mathbf{R}^2} g_l d\mu_l \to \int_{\partial\omega} g d\mu$$

as $l \to +\infty$, see [13] for the proof. Here we choose $l >> L$ for better accuracy.

Example 5.1: Let

$$\begin{aligned} \omega &= \{x^2 + y^2 \leq 5^2\} \\ \Omega &= \{|x|, |y| \leq 15\} \end{aligned}$$

$$\Lambda = \{(i,j) : i,j = -15 \cdot 2^L, \ldots, 15 \times 2^L - 5\},$$

and we want to solve

$$\Delta u + u = f, \quad \frac{\partial u}{\partial n} = g \quad \text{on } \partial\omega.$$

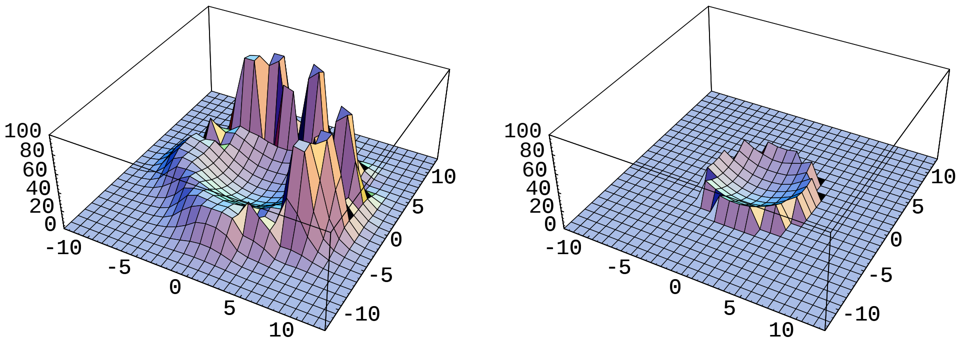

Figure 5.8: The wavelet Galerkin solution for $\epsilon = 10^{-3}$.

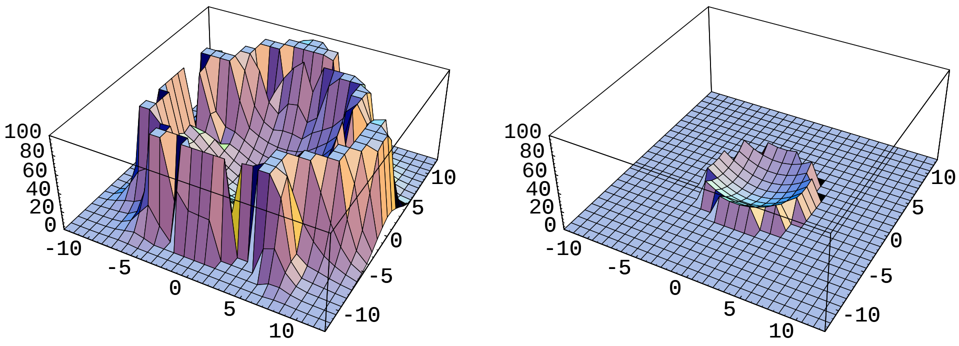

Figure 5.9: The wavelet Galerkin solution for $\epsilon = 10^{-6}$.

Time Consumed :	L	$=$	$0:$	15 minutes
	L	$=$	$1:$	168 minutes

Table 5.3: Comparative times on a SparcStation using Matlab coding

Here we assume that we use the order 3 translated Daubechies scaling functions as our basis. The test problem is chosen so that $u = x^2 + y^2$ is the desired solution. We solve for the numerical solution at level $L = 0, 1$. Once the linear system is set, we use the LU decomposition to solve it. In Figures 5.8, 5.9, and 5.10 we see graphs of solutions of the solution to this test problem for variable values of the regularizing parameter ϵ. In the following table we see a comparison of the time consumed for different levels, and in the following section we see a comparison with the finite element computations given in the previous section. In this paper we are more concerned with checking the accuracy of these methods. In later papers we will go to methods which will dramatically speed up these calculations yielding the same accuracy (such as multigrid and parallel computation; see [6], [11]).

In the following tables, we present the relative errors $E_\omega^{\epsilon,L}$ with respect to different choices of ϵ and the levels $L = 0, 1$, in H^1 and L^2 norm. More specifically, if we denote the wavelet solution by $u^{\epsilon,L}$, then

$$E_\omega^{\epsilon,L} := \frac{\|u^{\epsilon,L} - u\|_{L^2(\omega)}}{\|u\|_{L^2(\omega)}},$$

or

$$E_\omega^{\epsilon,L} := \frac{\|u^{\epsilon,L} - u\|_{H^1(\omega)}}{\|u\|_{H^1(\omega)}}.$$

These can be calculated numerically as follows.

Assume we have the expansions of $u^{\epsilon,L}$ and u^L at the level L. Also we suppose that χ_ω^L is the expansion of the characteristic function χ_ω of ω at level L. Then

$$\|u^{\epsilon,L} - u\|_{L^2(\omega)} = \|(u^{\epsilon,L} - u)\chi_\omega^L\|_{L^2(\omega)}.$$

Similarly, using connection coefficients for the first order derivative, one can

ϵ	$L=0$	$L=1$
10^{0}	0.72312811620280	0.70420788736429
10^{-1}	0.24079518419690	0.20971773207275
10^{-2}	0.69763698457707	0.13364955388352
10^{-3}	0.71127229550499	0.02133194677591
10^{-4}	0.02153308376562	0.13696729249436
10^{-5}	0.02418248442799	0.00968907358125
10^{-6}	0.02697287795870	0.00923777387524
10^{-10}	0.02491507164637	0.00934298716397

Table 5.4: Relative error in H^1 norm. $\|u^{\epsilon,L} - u\|_{H^1(\omega)}/\|u\|_{H^1(\omega)}$ for $u(x,y) = x^2 + y^2$ for wavelet method

calculate the expansions of

$$\frac{\partial(u^{\epsilon,L} - u^L)}{\partial x}, \frac{\partial(u^{\epsilon,L} - u^L)}{\partial y}$$

and

$$\frac{\partial u^L}{\partial x}, \frac{\partial u^L}{\partial y}.$$

Then

$$\|\frac{\partial}{\partial x}(u^{\epsilon,L} - u^L)\|_{L^2(\omega)} = \|\frac{\partial(u^{\epsilon,L} - u^L)}{\partial x}\chi_\omega^L\|_{L^2(\omega)},$$

etc.

In Figures 5.10, 5.11, and 5.12, we see comparison of these same solutions for slices near the middle of the fictitious domain Ω with respect to different ϵs.

5.3 Comparison of Finite Element and Wavelet Accuracy

In Table 6.6, the comparison between the numerical results obtained by wavelet method and those obtained by finite element method is presented with ϵ varying from 10^{-1} to 10^{-10}. Both methods have been applied to the

ϵ	$L=0$	$L=1$
$\epsilon=1$	0.64011168983714	0.60030587469127
10^{-1}	0.18728365752675	0.14122301303582
10^{-2}	0.06349181648207	0.02920589711123
10^{-3}	0.06433735001700	0.00359286263457
10^{-4}	0.00563482997730	0.00196723305079
10^{-5}	0.00280148379091	$4.461257406785745 \times 10^{-4}$
10^{-6}	0.00201636549800	$5.006539897281224 \times 10^{-4}$
10^{-10}	0.00192268309090	$5.194671480165910 \times 10^{-4}$

Table 5.5: Relative error in L^2 norm. $\|u^{\epsilon,L} - u\|_{L^2(\omega)}/\|u\|_{L^2(\omega)}$ for $u(x,y) = x^2 + y^2$ for wavelet method

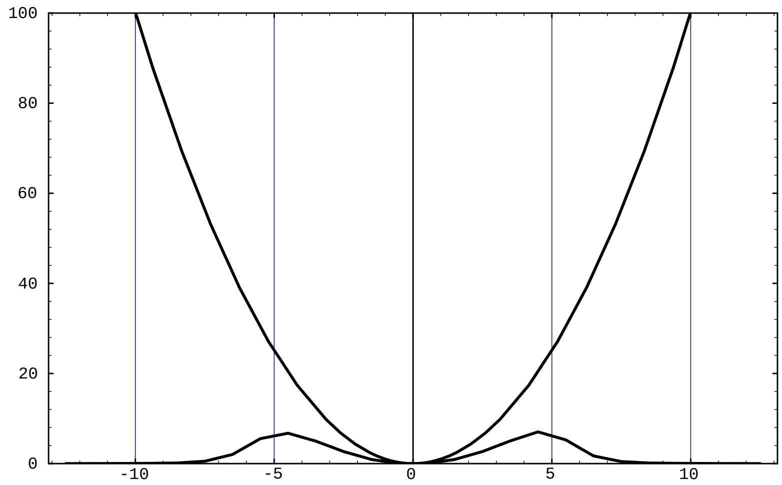

Figure 5.10: Solution u^ϵ, for $\epsilon = 1$, restricted to $y = 0$

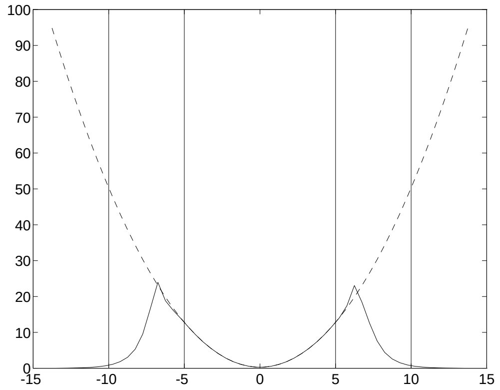

Figure 5.11: Solution u^ϵ, for $\epsilon = 10^{-4}$, restricted to $y = 0$

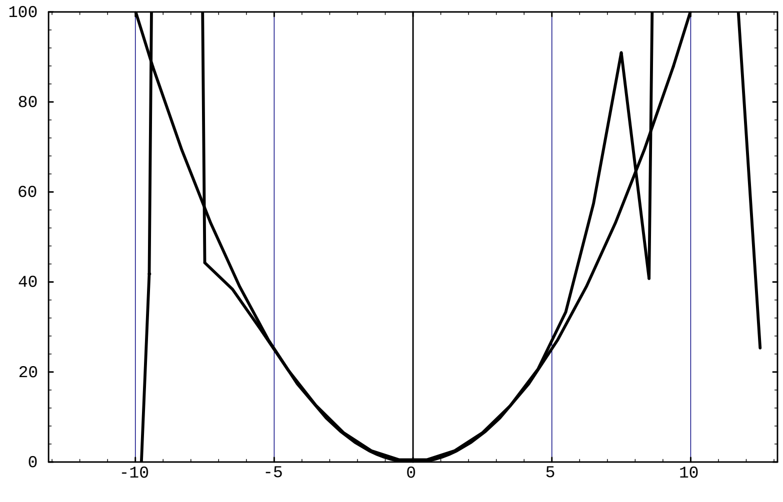

Figure 5.12: Solution u^ϵ, for $\epsilon = 10^{-6}$, restricted to $y = 0$

ϵ	wavelet	finite element
10^{-1}	0.19653	1.38506
10^{-2}	0.06411	0.34298
10^{-3}	0.32074	0.09031
10^{-4}	0.01717	0.14601
10^{-5}	0.05829	0.15172
10^{-6}	0.02049	0.15229
10^{-7}	0.01350	0.15235
10^{-8}	0.01349	0.15235
10^{-9}	0.01359	0.15236
10^{-10}	0.01359	0.15236

Table 5.6: Comparison of relative L^2 error obtained by wavelet method and finite element method.

same test problem

$$\begin{aligned} u - \Delta u &= x^2 + y^2 - 4 \text{ in } \omega, \\ \frac{\partial u}{\partial n} &= g \text{ on } \gamma, \end{aligned}$$

whose exact solution is $u(x,y) = x^2 + y^2$. For both methods, the geometry of the fictitious domain is the same, the mesh is the uniform mesh and the number of mesh points in x–direction and y–direction is 33. But the basis for wavelet method are genus 3 scaling functions and the finite diemnsional subspace for finite element method is the one defined in (5.2.2) which consists of piecewise continuous linear functions.

The better behavior of the relative L^2–error obtained by wavelet approximation is expected. In [9] it is pointed out that the approximation of the first order differential operator associated with the genus 3 Daubechies wavelet basis is the 9–point finite difference operator with trunction error of order 4. By Theorem 4.5, the finite element approxiamtion with piecewise continuous linear functions is of 2nd order.

Also in wavelet approximation, the part $\int_\omega (vw + \nabla v \cdot \nabla w)\, dxdy$ and the boundary integral are calculated systematically using the characteristic function χ_ω and its corresponding measure $-\nabla \chi_\omega \cdot \vec{\mathbf{n}}$. A parametriztion of the boundary curve was not required or used. Also in the computation of the

$\int_{\omega}(vw+\nabla v\cdot\nabla w)\,dxdy$ in the finite element approximation, we need to do it *accurately* over these elements T with area$(T\cap\omega)\neq 0$ and area$(T\cap\omega)\neq$area(T) in the triangulation of the fictitious domain Ω to obtain good results.

The numerical solutions of finite element method have no oscillation over the fictitious domain and approximate the solutions very well near the boundary of ω for small ϵ (see Figure 5.1 for instance). On the other hand the numerical solution of the wavelet method has significant oscillation outside the actual domain ω (see Figures 5.8, 5.9, and 5.12), which may be because of the approximation of the boundary integral.

6 Conclusion

In this paper we have seen that the wavelet-Galerkin method is comparable to the classical finite element problem, and has inherently more accuracy if linear finite elements are used. It is a simple matter to change the wavelet code to implement Daubechies coefficients of higher rank to get more accurate solutions, and of course, at a cost of slower running time. The principal difference between the two methods in this paper was in the coding for the integration around the boundary of the given domain ω. For the finite element method it was necessary to use an explicit parametrization of the boundary (in this case as a circle), and for the wavelet method the calculation of the boundary integral resulted from differentiating the characteristic function of the domain. For some problems in higher dimension the parametrization of the boundary would be more difficult and having code that computes such integrals automatically will be beneficial, although there is some cost in the implementation, but no cost in the coding time. One consequence of the work in this paper is that one sees that the fictitious domain method here works for the boundary of an essentially arbitrary bounded domain (with the assumption that the boundary is rectifiable), and as remarked above, there is a difference in the coding of the boundary integrals for both methods (requiring a knowledge of the parametrization of the boundary curve for the finite element method).

In future papers we will explore the extension of these ideas to the multigrid and parallel processing arena. The ultimate goal is to find a general solution method which involves multilevel localized analysis, doing calculations at different scales (or several scales at the same time a la multigrid) at different regions of the domain considered, depending on the nature of how much computational power one needs from one point to another.

References

[1] P. G. Ciarlet. Basic error estimates for elliptic problems. In P. G. Ciarlet and J. L. Lions, editors, *Handbook of Numerical Analysis, Vol II*. North-Holland, Amsterdam, 1991.

[2] Phillipe G. Ciarlet. *The finite element methods for elliptic problems*. North-Holland, 1987.

[3] I. Daubechies. Orthonormal bases of compactly supported wavelets. *Comm. Pure Appl. Math.*, 41:906–966, 1988.

[4] D. Gilbarg and N. S. Trudinger. *Elliptic partial differential equations of second order*. Springer-Verlag, Berlin, 1983.

[5] R. Glowinski and T. W. Pan. Error estimates for fictitious domain/penalty/finite element methods. *Calcolo*, 29:125–141, 1992.

[6] R. Glowinski, A. Rieder, R. O. Wells, and X. Zhou. A wavelet multigrid preconditioner for Dirichlet boundary value problems in general domains. Computational Mathematics Laboratory TR93-06, Rice University, 1993.

[7] Roland Glowinski. *Numerical Methods for Nonlinear Variational Problems*. Springer Series in Computational Physics. Springer-Verlag, New York, 1984.

[8] N. Kikuchi and J. T. Oden. *Contact Problems in Elasticity: A Study of Variational Inequalites and Contact Problems*. SIAM, Philadelphia, 1988.

[9] K. McCormick and R. O. Wells. Wavelet calculus and finite-difference operators. *Math of Comp*, 1993. To appear.

[10] J. L. Lions R. Glowinski and R. Tremolieres. *Numerical Analysis of Variational Inequalities*. North-Holland, Amsterdam, 1981.

[11] A. Rieder, R. O. Wells Jr., and X. Zhou. A wavelet approach to robust multilevel solvers for anisotropic elliptic problems. *Applied and Computational Harmonic Analysis*, 1994. To appear.

[12] Gilbert Strang and George J. Fix. *An analysis of the finite element method*. Prentice-Hall, Englewood Cliffs, NJ, 1973.

[13] R. O. Wells and Xiaodong Zhou. Wavelet solutions for the Dirichlet problem. Technical Report 92-02, Rice University, 1992. Computational Mathematics Laboratory.

[14] R. O. Wells and Xiaodong Zhou. Wavelet interpolation and approximate solutions of elliptic partial differential equations. In R. Wilson and E. A. Tanner, editors, *Noncompact Lie Groups*. Kluwer, 1994. To appear. Proceedings of NATO Advanced Research Workshop.